Original research

Effects of a micro-thread at the implant neck on securing the quantity and quality of bone formation around implants

Yinghui Li, Shin-ichi Yamada*, Hitoshi Aizawa, Fangfang Qi, Tetsu Shimane, Masafumi Morioka, Hiroshi Kurita

Department of Dentistry and Oral Surgery, Shinshu University School of Medicine, 3-1-1, Asahi, Matsumoto, 390-8621, Japan

* Correspondence to: Shin-ichi Yamada, DDS, PhD
Department of Dentistry and Oral Surgery
Shinshu University School of Medicine
3-1-1, Asahi, Matsumoto, 390-8621, Japan.
Tel.: +81 (0)263-37-2675, Fax: +81 (0)263-37-2676
E-mail: yshinshin@shinshu-u.ac.jp

Keywords: implant neck, osseointegration, macro-thread, micro-thread, osteoblast

Running title: Effects of a micro-thread at the implant neck on securing the quantity and quality of bone formation

Abstract

Objective: The purpose of this study was to examine the effects of different implant neck designs on securing the quantity and quality of peri-implant hard tissue during the period of healing after implant placement.

Materials and Methods: Three types of implants with different neck morphologies (no thread, a macro-thread, and a micro-thread) were placed in the femur and tibia of six adult male New Zealand white rabbits. After 3 and 8 weeks, animals were sacrificed and subjected to micro-computed tomography (CT) and histological assessments.

Results: All implants were clinically, radiographically, and histologically osseointegrated at the time of euthanasia. Micro-CT data revealed that the micro-thread design had a higher number and wider trabecular bone attachment than other implant designs after 3 and 8 weeks. The results of toluidine blue staining demonstrated that the percentages of bone-to-implant contact (%BIC) and new bone area (%NBA) were significantly higher with type C than with the other types after 3 weeks. After 8 weeks, the %NBA of type C was higher than that of type A.

Conclusion: Our results suggest that an implant with a micro-thread at the implant neck promotes faster osteogenesis and a greater amount of new bone around the implant.

1. Introduction

Implant therapy is regarded as a safe and reliable method for patients with complete or partial edentulism [1,2]. While the current 5-year survival rate of modern titanium implants is greater than 95%, their success in elderly and compromised patients is significantly lower [3-5]. There are two main causes of implant failure: biological and mechanical. The quantity and quality of bone supporting dental implants are some of the key factors that influence implant success [6,7].

Previous studies demonstrated that the surface geometry of an implant is a key factor affecting the implant success rate [8-10]. Implants with a rough surface have been shown to stimulate more bone formation, directly influencing the behavior of bone-forming cells by a mechanical stimulation and interactions with the intracellular signaling pathways mediated by focal adhesions [11]. Furthermore, a close relationship has been reported between marginal bone loss and implant surface characteristics [12,13]. A dental implant design with horizontal grooves or mini-threads near the top of the implant is known to reduce marginal bone loss [12,14,15]. Based on finite element studies, Hansson and Norton suggested the use of optimal minute threads at the implant neck in implants because they may prevent stress concentration in the implant and bone interface and simultaneously provide suitable stresses to maintain osseointegration [16,17]. However, few studies have evaluated the effects of different implant neck designs on bone formation [18].

The formation of new bone mainly occurs by the deposition of a bone matrix secreted by osteoblasts. Osteopontin has been implicated as an important factor in bone remodeling. Osteopontin is a multifunctional phosphorylated glycoprotein secreted by osteoblasts, and has been suggested to occur at early stage during bone development and to promote attachment of osteoblasts to the extracellular matrix[19]. It plays also a role in anchoring osteoclasts to the mineral matrix of bones [20]. Osteocalcin is a marker of bone formation, vitamin K and vitamin D dependent protein, produced by osteoblasts[21].

Therefore, the aim of the present study was to examine the effects of different implant neck designs on securing the quantity and quality of peri-implant hard tissue after implant placement using a histomorphometric analysis.

2. Materials and Methods

2.1. Implant neck design

Three types of endoosseous titanium implants with different neck morphologies, but the same blast surface (neck diameter 2.9 mm and body length 3.5 mm, with the same body thread, manufactured by Yoshioka Co., Ltd., Nagano, Japan) were used in the present study (Figure 1).

Type A: No thread at the implant neck.

Type B: A macro-thread at the implant neck (valley diameter 2.7 mm, depth of the thread 0.3 mm, and thread pitch 0.7 mm).

Type C: A micro-thread at the implant neck (valley diameter 2.7 mm, depth of the thread 0.1 mm, thread pitch 0.1 mm, and thread angle 60°).

2.2. Surgical procedure and study protocol

Six male New Zealand white rabbits (age: 6 months, weight: 3.5–4.0 kg) were used in the present study. Implants were placed in the femur and tibia of the rabbits; one implant in the distal femoral condyle and two implants in the proximal tibial metaphysis alternatively. Thirty-six implants were placed in 6 rabbits. Under general anesthesia induced by 3% pentobarbital (30 mg/kg/i.v.; Somnopentyl; Kyoritsu Seiyaku, Japan) and 2% lidocaine (1 ml i.m.; AstraZeneca, Osaka, Japan), all implants were placed at 35Ncm following the manufacturer's guidelines with a 2.5-mm final drill and primary close sutures. Postoperatively, each animal received penicillin to prevent infection (50000 IU/kg on the day of surgery and for the next 3 days). After 3 and 8 weeks, animals (n=3) were sacrificed by an overdose of pentobarbital, all implants and surrounding bone tissue were retrieved *en bloc*, fixed by immersion in 10% neutral buffered formalin, and subjected to radiological and histological assessments.

All experimental protocols were approved by the Shinshu University Animal Care and Use Committee.

2.3. Radiological assessment (Micro-computed tomography (CT))

Specimens including the implants were assessed by high-resolution micro-CT (RmCT; i-VIEW-R 1.26, Rigaku, Tokyo, Japan) using an X-ray source set at 80 kV and 80A over an angular range of 360° with a magnification of 4. At a representative vertical central image of the implant, trabecular bone attachments to the lateral surface of the implant (TBN; trabecular bone number per implant height, TBT; trabecular bone thickness, and TBS; trabecular bone separation (mm) as the distance between trabecular bones) were assessed (Figure 2). All counts and measurements (to the second decimal point in mm) were performed three times at different time points with a random sample order and average values were calculated.

2.4. Histological assessment

The samples retrieved from the tibias were dehydrated in a graded series of ethanol and embedded in light-curing resin (Technovit 7200 VLC, Kulzer, Wehrheim, Germany). Cut and ground sections were prepared from the embedded blocks with a final thickness of 30 μm, and then stained with 1% toluidine blue. Sections at a representative vertical center of the implant were observed using a light microscope (Biorevo BZ-9000, Keyence, Osaka, Japan). After digitizing the image of each specimen, the percentage of bone-to-implant contact (%BIC; mm of bone contact/implant height) and the percentage of new bone area (%NBA; mm of newly formed bone/implant height) were measured using ImageJ and Image Pro plus (Media Cybernetics Inc, Bethesda, MD, USA). All measurements were conducted three times at different time points with a random sample order, and average values were calculated.

2.5. Immunohistological analysis

The samples retrieved from femurs were decalcified in 10% EDTA for two months. After removing the implants, bone samples were dehydrated in a graded series of ethanol and embedded in paraffin. Vertically cut sections at the representative center of the implant were prepared from embedded blocks with

a final thickness of 5 μm for immunohistochemical staining.

The appearance of the osteoblast differentiation markers osteopontin and osteocalcin within the healing bone was assessed using the corresponding antibody (anti-osteopontin antibody O7264, Sigma-Aldrich, St. Louis, USA; anti-osteocalcin antibody ab13418, Abcam, Cambridge, UK). After deparaffinization and hydration, slices were fixed in 3% hydrogen peroxide formaldehyde solution at room temperature for 30 minutes in order to block endogenous peroxidase reactivity, and were then incubated with primary antibodies and diluted anti-osteopontin antibody (1:200) or anti-osteocalcin antibody (1:100) at 4°C overnight. After the sections were rinsed with Tris-HCL Buffer Saline (TBS), they were incubated with an anti-rabbit/mouse secondary antibody at room temperature for 30 minutes. After rinsing with TBS, sections were treated with 3-3'-diaminobenzidine tetrahydrochloride (DAB) solution to visualize the reaction product. Positive cells near the implant bone interface were counted three times at different time points with a random sample order, and average numbers (per mm) were calculated.

2.6. Statistical analysis

Statistical analyses were performed using Graphpad Prism 6 (Graphpad Software, California, USA). The Kruskal-Wallis and Dunn's multiple comparison tests were performed in order to evaluate differences between implant types. P-values <0.05 were considered to be significant.

3. Results

3.1. Radiological analysis

Representative micro-CT samples are shown in Figure 2. All implants were surrounded by bone tissue. The results of measurements for TBN, TBT, and TBS are shown in Figure 3. Three weeks after implantation, type C had significantly higher mean values for TBN and TBT than type A or B (the Kruskal-Wallis and Dunn's multiple comparison tests, $p < 0.05$). Regarding TBS, type C had a significantly lower mean value than type A or B (the Kruskal-Wallis and Dunn's multiple comparison tests, $p < 0.05$).

After 8 weeks, type C showed higher mean values for TBN and TBT as well as a lower mean value for TBS than type A or B, and the differences in TBN and TBT between types B and C and in TBS between types A and C were significant (the Kruskal-Wallis and Dunn's multiple comparison tests, $p < 0.05$).

3.2. Histological analysis

Representative histological samples are shown in Figure 4. Complications, such as allergic reactions, abscesses, or infections, were not observed in any of the specimens tested. After 3 weeks, osteogenetic activity peaked and large amounts of new bone were observed. There were clear boundaries between new bone and old cortical bone. After 8 weeks, the new bone mass had increased and matured.

The results of the assessments of %BIC and %NBA are shown in Figure 5. Three weeks after implantation, Type C showed significantly higher mean %BIC as well as %NBA than type A or B (the Kruskal-Wallis and Dunn's multiple comparison tests, $p < 0.05$). At 8 weeks, type C showed higher mean values for %BIC and %NBA than type A or B, and the difference in %NBA between types A and type C was significant (the Kruskal-Wallis and Dunn's multiple comparison tests, $p < 0.05$).

3.3. Immunohistochemical analysis

The removed implants were observed by scanning electron microscopy (SEM) and revealed that only sporadic bone tissue remained on the implant surface. In immunohistochemical staining, selected images demonstrating immunoreactivities for osteopontin and osteocalcin, as indicated by brown cellular staining, are shown in Figure 6. Staining showed that a large number of brown-stained osteoblasts were located at the bone-implant interface, particularly at the valley of the micro-threads. The positive cell numbers for osteopontin and osteocalcin were also summarized in Figure 6. Three weeks after implantation, type C had more positive cells for osteopontin and osteocalcin than type A or B. Eight weeks after implantation, type C still had more positive cells for osteocalcin than the other two types. However, the number of samples for immunohistochemical staining (n=2) was too small for a statistical analysis between the types.

4. Discussion

The use of dental implants has become an integral part of modern dentistry. Since the introduction of implants, related research has not ceased. Most studies focus on how to achieve high-quality osseointegration as soon as possible [22]. Previous studies have focused on the texture of the implant surface, and the findings obtained showed that a rough surface may promote the growth of new bone [8,9,11]. On the other hand, macro-morphology has been suggested as one of the key factors affecting implant success [10,18]. In order to assess the influence of macro-morphology, particularly at the implant neck, and exclude the possible effects of the micro-topography of the implant surface, three types of different neck implant macro-designs with the same roughened surface were compared in the present study.

The present results showed that type C had a significant advantage for new bone formation and a subsequent increase in implant-to-bone contact. Three weeks after implantation, type C showed significantly greater new bone formation (%NBA) and a larger area of bone implant contact (%BIC) than types A and B. This result was consistent with those obtained in the radiological assessment, which showed the type C secured a significantly higher number (TBN) and amount of trabecular bone (TBT) at the implant-bone interface than types A and B. At 8 weeks, although the advantages of type C remained, they were less pronounced. Chowdhary et al. implanted two different macrogeometry-modified implants (a macro-thread only vs. a micro-thread between the macro-threads) in the rabbit tibia for four weeks and a histological assessment revealed no significant differences in NBA and BIC between these implants [10]. These findings were not in agreement with our results. We speculated that this disagreement may have been due to differences in the implant macro-design employed. In Chowdhary's study, a micro-thread was designed between macro-threads and, thus, there was a wide gap between the micro-thread and bone surface of the prepared implant cavity. On the other hand, in the present study, we employed a tapered implant design and a micro-thread was created at the implant neck; therefore, the micro-thread made mechanical contact with the surrounding bone surface (Fig. 7). During implant placement, since the

diameter of the implant hole is generally smaller than that of the implant, the threads become embedded in the bone, resulting in high primary stability [23]. Due to the extrusion of micro-threads, some closed micro-chambers are created between the implant threads and surrounding bone, which allows blood to be held within the chamber and results in bone formation [24,25]. In the present study, we inferred that type C had more micro-chambers in the neck part, which may be an important factor triggering new bone formation. Therefore, we speculate that type C achieves faster and greater %BIC and %NBA than the other types.

The formation of new bone mainly occurs by the deposition of a bone matrix secreted by osteoblasts. In normal bone tissue metabolism, osteoblasts interact with osteoclasts and achieve an equilibrium state. However, when the implant is inserted into the bone, bone tissue injury will activate osteoclasts and lead to bone resorption. The activity of osteoclasts, in turn, activates osteoblasts and bone formation, which is the switch from mechanical to biological stability. Osteopontin and osteocalcin are secreted by osteoblasts and play important roles in new bone formation[19-21]. Therefore, in the present study, the activation of osteoblasts was assessed using the bone biomarkers osteopontin and osteocalcin. In the present study, although a statistical analysis was not performed, the number of osteoblasts in type C appeared to be higher than those of the other types at 3 weeks. Toluidine blue staining showed that the micro-thread type may achieve greater and faster increases in %BIC and %NBA; therefore, there may have been more osteoblasts in type C because the new bone was produced by osteoblasts. Although we did not investigate the underlying cellular pathway mechanism, previous studies showed that new vessels will arise near the implant surface in the concavities between the threads after implantation, thereby creating a rich blood supply that is beneficial to osteoblasts and new bone formation [26].

One of the most important functions of the threads of implants is to provide primary stability. The primary stability of an implant is regarded as an important factor for achieving osseointegration and assessing the timing of prosthetic loading [27]. Primary stability is achieved by a mechanical engagement between the implant and host bone at the time of implant placement. Thus, implant macro-design (e.g.,

geometry, length, and diameter) and bone quantity and quality influence primary stability. In the present study, due to the characteristics of rabbit legs, there was more cortical bone near the surface and more cancellous bone in the center of the leg. Therefore, primary stability may be provided by cortical bone. Cortical bone influences the primary stability of the implant and the subsequent osteogenic reaction [28]. In the present study, the primary stabilities of types B and C were markedly higher than that of type A, and this may have been because there were more threads on the necks of the two types of implants. A previous study reported that decreasing the thread pitch may positively influence initial mechanical stability [29]. We speculated that in contrast to the macro-thread and no thread surface, the micro-thread clearly provides better primary implant stability, which may also be beneficial for successful bone formation.

Previous studies suggested that a micro-thread on the implant neck is a key feature for successful implant treatment. Peri-implant bone loss was found to be reduced around implants with micro-threads at the implant neck [31,32]. The use of micro-threads in the neck region is being recognized as an efficient strategy to organize the transmitted stress through cortical bone. Micro-threads are considered to increase the axial stiffness of the implant and decrease shearing stresses in cortical bone more than standard threads, which may positively contribute to maintaining the bone crest surrounding the implant [33,34]. However, the effects of micro-threads located at the implant neck on securing the quality and quantity of osteogenesis around the implant currently remain unknown. The results of the present study showed that an implant with a micro-thread at the implant neck may promote faster osteogenesis and a greater amount of new bone around the implant after implant placement. Micro-threads at the implant neck secured primary implant stability and more rapidly induced a larger amount of new bone formation around the implant, which may be favorable for achieving early osseointegration and less peri-implant bone loss.

The strength of the present study was that it examined the effects of implant neck design on early osteointegration. The limitation of this study was that the number of samples for immunohistochemical staining (n=2) to demonstrate immunoreactivity for osteopontin and osteocalcin was too small for a statistical analysis between the implant types.

5. Conclusion

The results of the present study suggest that an implant with a micro-thread at the implant neck promotes faster osteogenesis and a greater amount of new cortical bone around the implant. A micro-thread at the implant neck contributes not only to reducing peri-implant bone loss, but also promoting osteogenesis around the implant

Acknowledgments

The authors are grateful to the team at the Department of Oral Surgery, Matsumoto Dental University, who provided guidance in experimental technology.

Author Contributions

Yinghui Li: Concept/Design, Experimental operating, Data analysis, Article writing

Shin-ichi Yamada: Data analysis/interpretation, Critical revision of the article

Hitoshi Aizawa: Experimental operating, Statistical analysis, Data collection

Fangfang Qi: Experimental operating, Data collection, Drafting the article

Tetsu Shimane: Experimental operating, Data collection

Masafumi Morioka: Experimental operating, Data collection

Hiroshi Kurita: Concept/Design, Critical revision of the article, Approval of the article

Disclosure of conflicts of interest

The authors state that they have no conflicts of interest.

Funding

This research did not receive any specific grant from funding agencies in the public, commercial, or

not-for-profit sectors.

References

[1] Levin L, Halperin-Sternfeld M. Tooth preservation or implant placement: a systematic review of long-term tooth and implant survival rates. J Am Dent Assoc 2013; 144: 1119-33.

[2] Engquist B, Nilson H, Astrand P. Single-tooth replacement by osseointegrated Branemark implants. A retrospective study of 82 implants. Clin Oral Implants Res 1995;6: 238-45.

[3] Shiffler K, Lee D, Rowan M, Aghaloo T. Effect of length, diameter, intraoral location on implant stability. Oral Surg Oral Med Oral Pathol Oral Radiol 2016;122:e193-8.

[4] Diz P, Scully C, Sanz M. Dental implants in the medically compromised patient. J Dent 2013; 41: 195-206.

[5] Matarasso S, Rasperini G, Iorio Siciliano V, Salvi GE, Lang NP, Aglietta M. A 10-year retrospective analysis of radiographic bone-level changes of implants supporting single-unit crowns in periodontally compromised vs. periodontally healthy patients. Clin Oral Implants Res 2010;21:898-903.

[6] Pjetursson BE, Thoma D, Jung R, Zwahlen M, Zembic A. A systematic review of the survival and complication rates of implant-supported fixed dental prostheses (FDPs) after a mean observation period of at least 5 years. Clin Oral Implants Res 2012; 23:22-38.

[7] Bozini T, Petridis H, Garefis K, Garefis P. A meta-analysis of prosthodontic complication rates of implant-supported fixed dental prostheses in edentulous patients after an observation period of at least 5 years. Int J Oral Maxillofac Implants 2011; 26:304-18.

[8] Brunette DM, Chehroudi B. The effects of the surface topography of micromachined titanium substrata on cell behavior in vitro and in vivo. J Biomech Eng 1999; 121: 49–57.

[9] Davies JE. Understanding peri-implant endosseous healing. J Dent Educ 2003; 67: 932–49.

[10] Chowdhary R, Jimbo R, Thomsen CS, Carlsson L, Wennerberg A. The osseointegration stimulatory effect of macrogeometry-modified implants: a study in the rabbit. Clin Oral Implants Res 2014; 25:1051-5.

[11] Dalby MJ. Cellular response to low adhesion nanotopographies. Int J Nanomedicine 2007; 2: 373-81.

[12] Gultekin BA, Sirali A, Gultekin P, Yalcin S, Mijiritsky E. Does the Laser-Microtextured Short Implant Collar Design Reduce Marginal Bone Loss in Comparison with a Machined Collar? Biomed Res Int. 2016;2016:9695389. Epub 2016 Aug 31.

[13] Niu W, Wang P, Zhu S, Liu Z, Ji P. Marginal bone loss around dental implants with and without microthreads in the neck: A systematic review and meta-analysis. J Prosthet Dent 2017 ;117:34-40.

[14] Song DW, Lee DW, Kim CK, Park KH, Moon IS. Comparative analysis of peri-implant marginal bone loss based on microthread location: a 1-year prospective study after loading. J Periodontol 2009; 80:1937-44.

[15] Abrahamsson I, Berglundh T. Tissue characteristics at microthreaded implants: An experimental study in dogs. Clin Implant Dent Relat Res 2006; 8:107-13.

[16] Hansson S. A conical implant-abutment interface at the level of the marginal bone improves the distribution of stresses in the supporting bone, an axisymmetric finite element analysis. Clin Oral Implants Res 2004; 14: 286–93.

[17] Norton M. Marginal bone levels at single tooth implants with a conical fixture design. The influence of surface macro-and microstructure. Clin Oral Implants Res 1998; 9: 91–9.

[18] Rasmusson L, Kahnberg KE, Tan A. Effects of implant design and surface on bone regeneration and implant stability: An experimental study in the dog mandible. Clin Implant Dent Relat Res 2001; 3:2-8.

[19] Sasano Y, Zhu JX, Kamakura S, Kusunoki S, Mizoguchi I, Kagayama M. Expression of major bone extracellular matrix proteins during embryonic osteogenesis in rat mandibles. Anat Embryol (Berl) 2000 ;202:31-7.

[20] Reinholt FP, Hultenby K, Oldberg A, Heinegård D. "Osteopontin--a possible anchor of osteoclasts to bone". Proc. Natl. Acad. Sci. U.S.A 1990;87: 4473–5.

[21] Lee AJ, Hodges S, Eastell R. Measurement of osteocalcin. Ann Clin Biochem 2000;37:432-446.

[22] Vasak C, Busenlechner D, Schwarze UY, Leitner HF, Munoz Guzon F, Hefti T, et al. Early bone

apposition to hydrophilic and hydrophobic titanium implant surfaces: a histologic and histomorphometric study in minipigs. Clin Oral Implants Res 2014; 25:1378-85.

[23] Natali AN, Carniel EL, Pavan PG. Investigation of viscoelastoplastic response of bone tissue in oral implants press fit process. J Biomed Mater Res B Appl Biomater 2009; 91: 868–75.

[24] Leonard G, Coelho P, Polyzois I, Stassen L, Claffey N. A study of the bone healing kinetics of plateau versus screw root design titanium dental implants. Clin Oral Implants Res 2009; 20: 232–9.

[25] Coelho PG, Suzuki M, Guimaraes MV, Marin C, Granato R, Gil JN, et al. Early bone healing around different implant bulk designs and surgical techniques: a study in dogs. Clin Implant Dent Relat Res 2010; 12: 202–8.

[26] Scarano A, Perrotti V, Artese L, Degidi M, Degidi D, Piattelli A, et al. Blood vessels are concentrated within the implant surface concavities: a histologic study in rabbit tibia. Odontology 2014; 102:259-66.

[27] Roccuzzo M, Aglietta M, Cordaro L. Implant loading protocols for partially edentulous maxillary posterior sites. Int J Oral Maxillofac Implants 2009; 24 : 147-57.

[28] Pommer B, Hof M, Fädler A, Gahleitner A, Watzek G, Watzak G. Primary implant stability in the atrophic sinus floor of human cadaver maxillae: impact of residual ridge height, bone density, and implant diameter. Clin Oral Implants Res 2014; 25:e109-13.

[29] Steigenga J, Al-Shammari K, Misch C, Nociti FH Jr, Wang HL. Effects of implant thread geometry on percentage of osseointegration and resistance to reverse torque in the tibia of rabbits. J Periodontol 2004;75:1233–41.

[30] Song DW, Lee DW, Kim CK, Park KH, Moon IS. Comparative analysis of peri-implant marginal bone loss based on microthread location: a 1-year prospective study after loading. J Periodontol. 2009;80:1937-44.

[31] Lee DW, Choi YS, Park KH, Kim CS, Moon IS. Effect of microthread on the maintenance of marginal bone level: A 3-year prospective study. Clin Oral Implants Res 2007;18:465-70.

[32] Schrotenboer J, Tsao YP, Kinariwala V, Wang HL. Effect of microthreads and platform switching on

crestal bone stress levels: a finite element analysis. J Periodontol. 2008;79:2166-72.

[33] Hudieb MI, Wakabayashi N, Kasugai S. Magnitude and direction of mechanical stress at the osseointegrated interface of the microthread implant. J Periodontol 2011;82:1061-70.

Figure legends

Figure 1. Three type of implants used in this study (The upper part is the schematic and the lower part is SEM micrographs of the implant neck surface 200×)

Type A: the neck with only a blast surface without a thread (A, D)

Type B: the neck and body with a macro-thread (B, E)

Type C: the neck with a micro-thread (C, F)

Figure 2. Representative images by micro-CT.

After healing, all implants were surrounded by bone tissue (A; Type A, B; Type B, and C; Type C)

The trabecular bone number (TBN), trabecular bone thickness (TBT), and trabecular bone separation (TBS) at the implant-bone interface were calculated using a micro-CT image (D).

Figure 3. Comparison of average trabecular bone number (TBN), trabecular bone thickness (TBT), and trabecular bone separation (TBS) among different implant neck designs

Type A: no thread, Type B: a macro-thread, and Type C: a micro-thread

*: the Kruskal-Wallis and Dunn's multiple comparison tests, $p < 0.05$

Figure 4. Descriptive light micrographs of magnified sections of implants 3 (the upper part) and 8 weeks (the lower part) after implantation

Type A: no thread, Type B: a macro-thread, and Type C: a micro-thread

Newly formed bone was observed near the implant-bone interface. NB, new bone; TB, trabecular bone; BM, bone marrow. Toluidine blue 4×

Figure 5. Comparison of the bone implant contact ratio (%BIC) and new bone area ratio (%NBA) after 3 and 8 weeks of healing.

Type A: no thread, Type B: a macro-thread, and Type C: a micro-thread

*: the Kruskal-Wallis and Dunn's multiple comparison tests, $P<0.05$

Figure 6. Immunohistochemical staining of osteoblast differentiation markers osteopontin (the upper part) and osteocalcin (the lower part)

Type A: no thread, Type B: a macro-thread, and Type C: a micro-thread

Positive proliferating cells stained brown/black within healing tissues near the implant-bone interface (arrow), particularly in the valley of the micro-thread (arrow head). 40×

Figure 7. Macro- and micro-thread designs employed in Chowdhary's study (A) and the present study (B)

Figures and tables

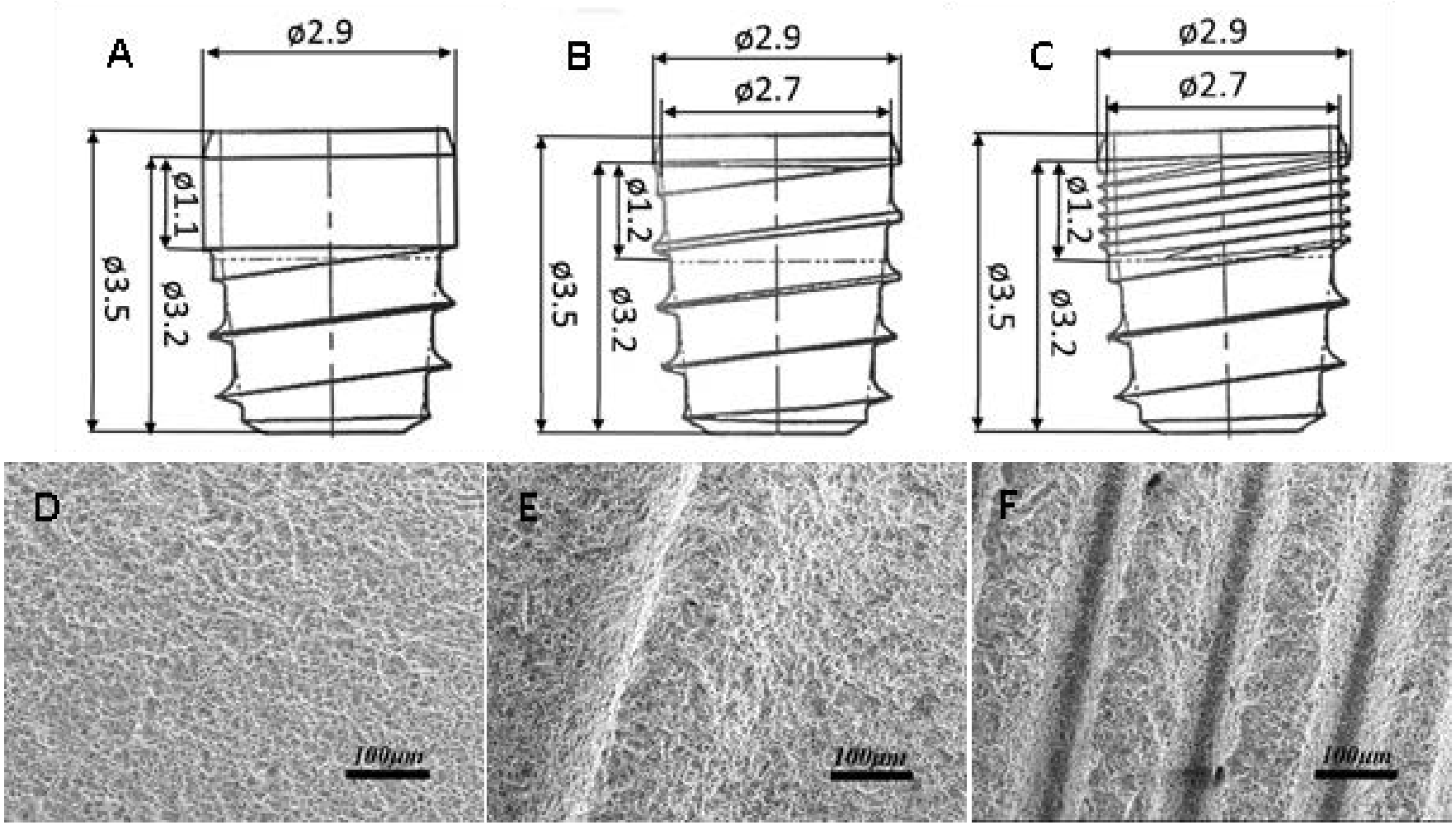

Figure 1. Three type of implants used in this study (The upper part is the schematic and the lower part is SEM micrographs of the implant neck surface 200 x)
Type A: the neck with only blast surface without thread (A, D)
Type B: the neck and body with macro-thread (B, E)
Type C: the neck with micro-thread (C, F)

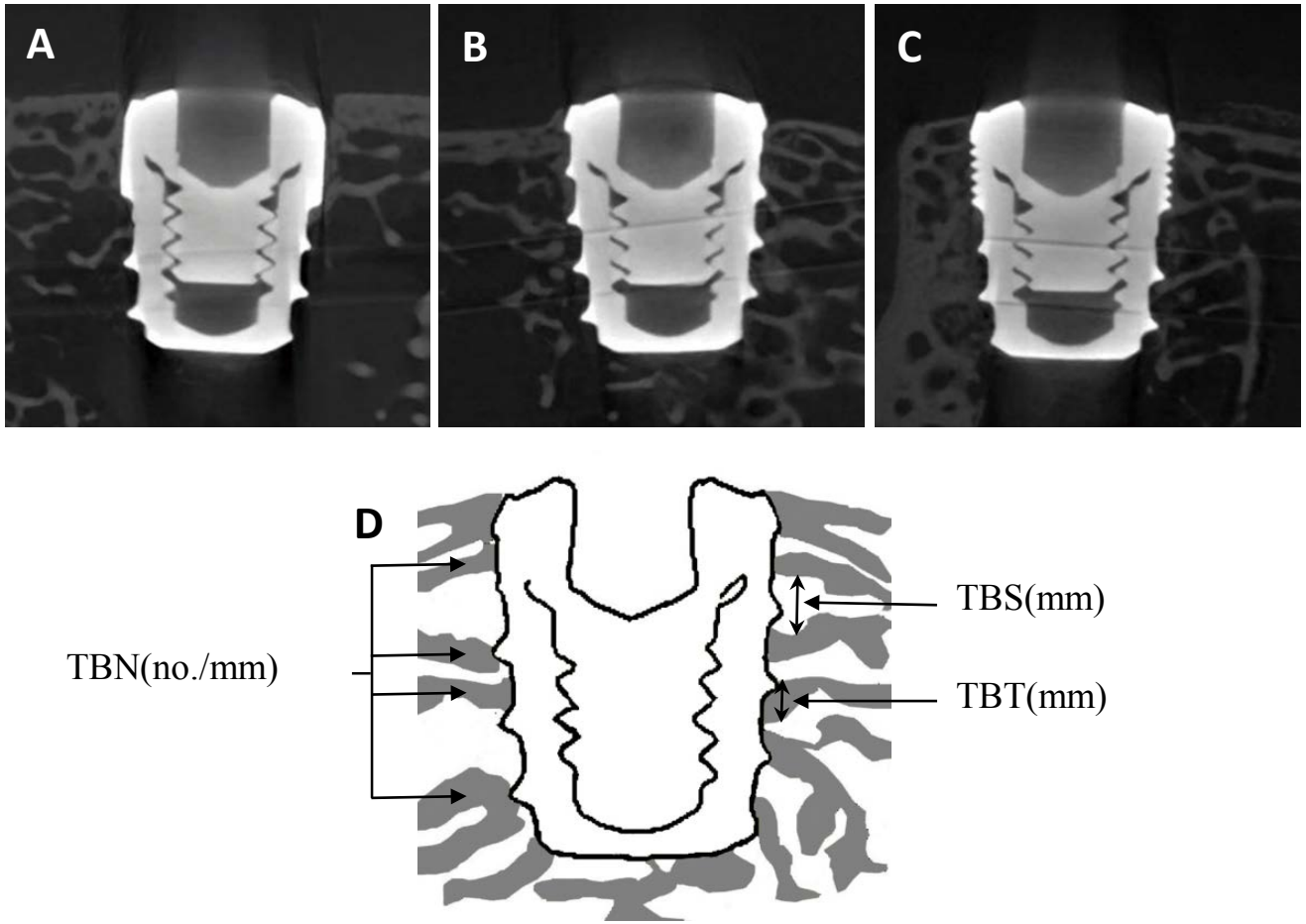

Figure 2. Representative images by micro CT.
After healing, all implants were surrounded by bone tissue (A; Type A, B; Type B, and C; Type C) Trabecular bone number (TBN), trabecular bone thickness (TBT) and trabecular bone separation (TBS) at the implant-bone interface were calculated using micro CT image (D).

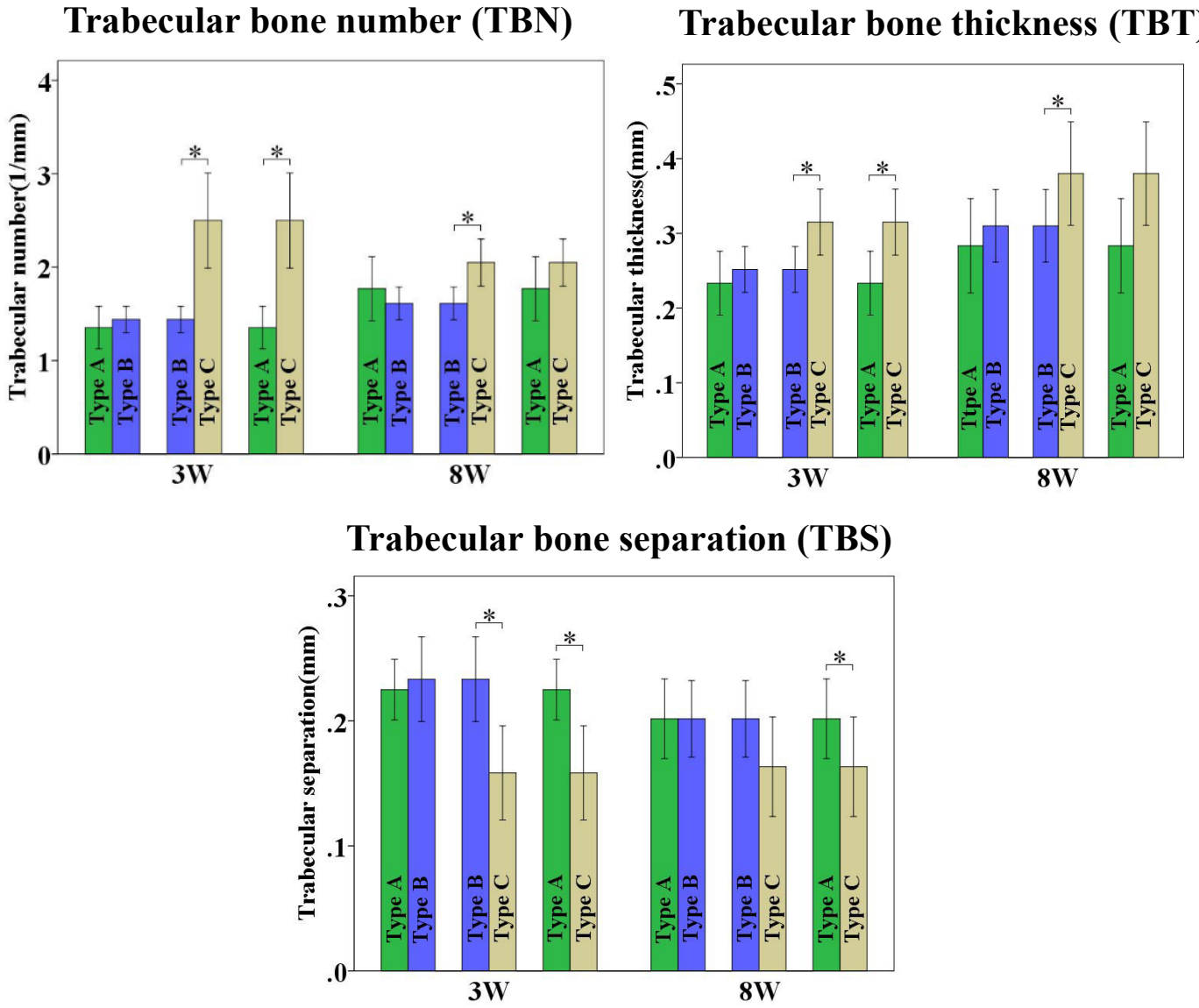

Figure 3. Comparison of average of trabecular bone number (TBN), trabecular bone thickness (TBT), and trabecular bone separation (TBS) among different implant neck designs

Type A: no thread, Type B: macro-thread, and Type C: micro-thread

*: Kruskal-Wallis with Dunn multiple comparisons test, $p < 0.05$

	3 weeks after implantation			8 weeks after implantation		
	Type A (n=4)	**Type B**	**Type C**	**Type A**	**Type B**	**Type C**
Trabecular bone number (no./mm)	**1.35 ± 0.23**	**1.44 ± 0.14**	**2.50 ± 0.51**	**1.77±0.34**	**1.61±0.17**	**2.05 ±0.25**
Trabecular bone thickness (mm)	**0.23 ± 0.04**	**0.25 ± 0.03**	**0.32 ± 0.04**	**0.28±0.06**	**0.31±0.05**	**0.38±0.07**
Trabecular bone separation (mm)	**0.23 ± 0.02**	**0.23 ± 0.03**	**0.16 ± 0.04**	**0.20±0.03**	**0.20±0.03**	**0.016±0.04**

Table 1 Comparison of average of trabecular bone number (TBN), trabecular bone thickness (TBT), and trabecular bone separation (TBS) among different implant neck designs

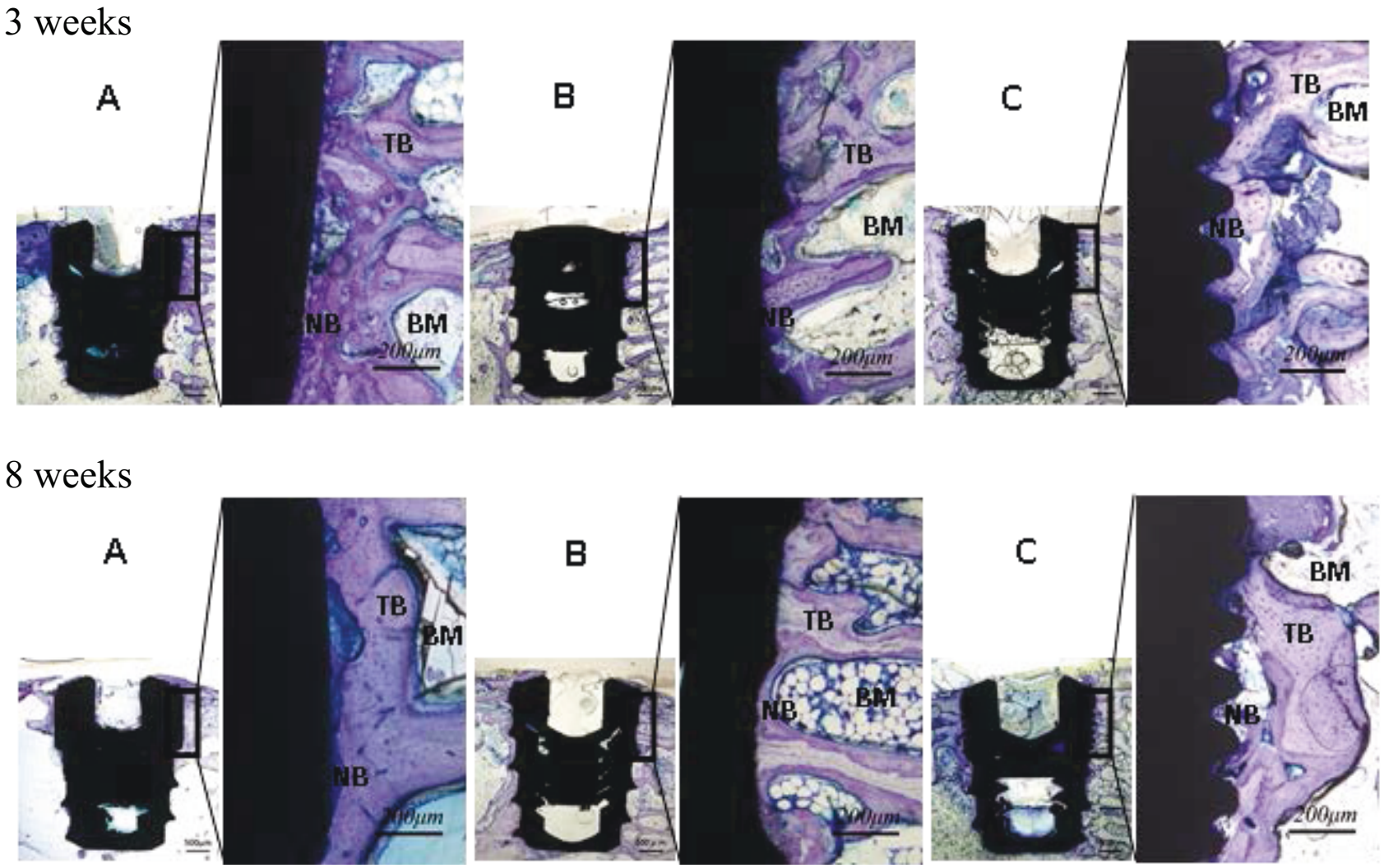

Figure 4. Descriptive light micrographs of magnified sections of the implants after 3 (the upper part) and 8 weeks (the lower part) after implantation

Type A: no thread, Type B: macro-thread, and Type C: micro-thread

Newly formed bone can be observed near the implant-bone interface. NB, new bone; TB, trabecular bone; BM, bone marrow. Toluidine blue 4×

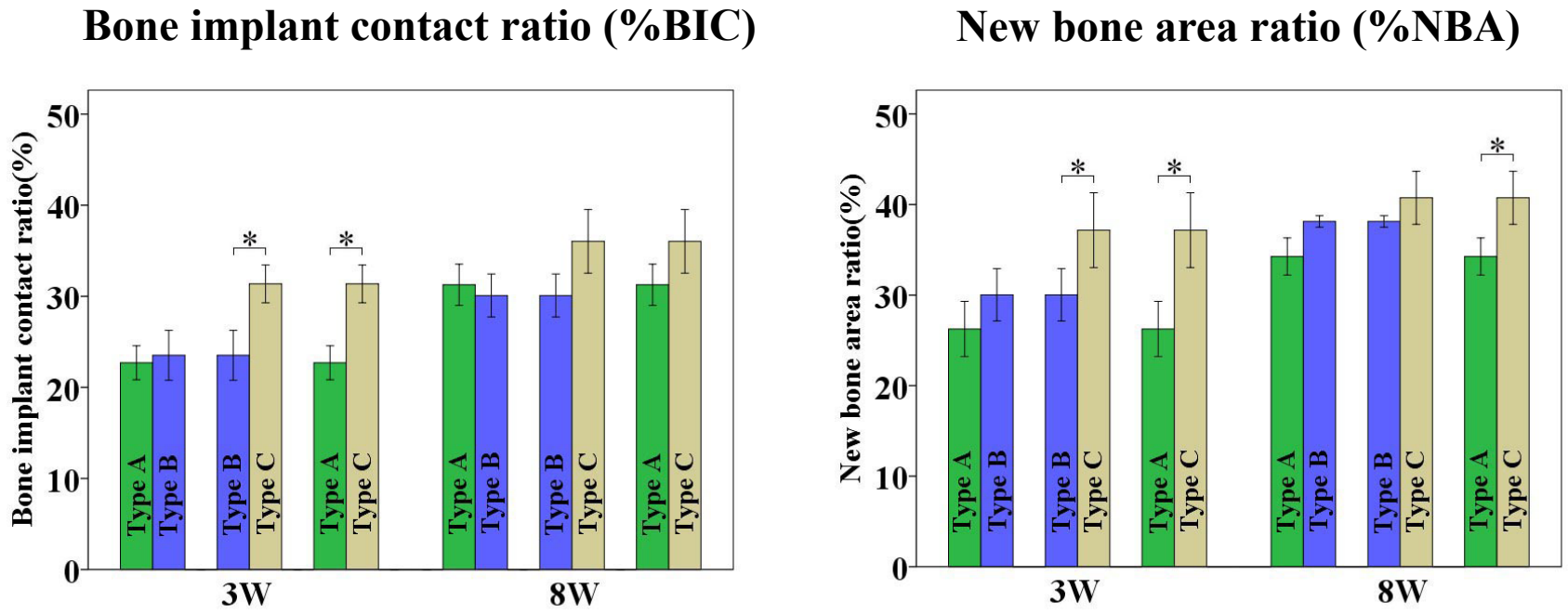

Figure 5. Comparison of bone implant contact ratio (%BIC) and new bone area ratio (%NBA) after 3 and 8 weeks of healing.
Type A: no thread, Type B: macro-thread, and Type C: micro-thread
*: Kruskal-Wallis with Dunn multiple comparisons test, $P<0.05$

	3 weeks after implantation			8 weeks after implantation		
	Type A (n=4)	**Type B**	**Type C**	**Type A**	**Type B**	**Type C**
Bone implant concact ratio (%)	**23.36 ± 3.1**	**24.51 ± 4.20**	**32.24 ± 3.76**	**30.93 ± 3.65**	**30.67 ± 3.17**	**36.08 ± 4.81**
New bone area ratio (%)	**26.52 ± 3.7**	**29.58 ± 3.37**	**37.15 ± 5.29**	**34.85 ± 4.52**	**38.58 ± 1.53**	**40.65 ± 3.89**

Table 2 Comparison of bone implant contact ratio (%BIC) and new bone area ratio (%NBA) after 3 and 8 weeks of healing

Osteopontin

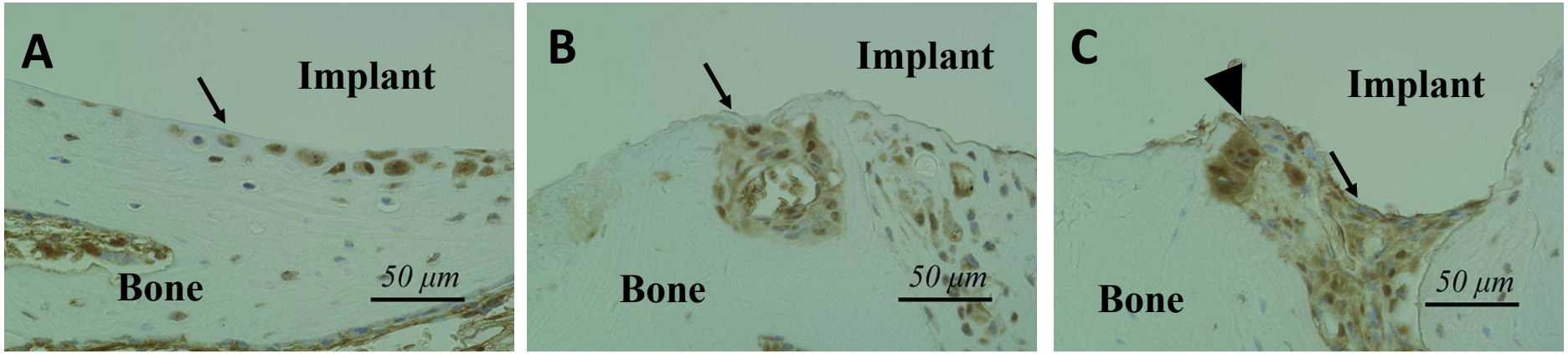

Osteocalcin

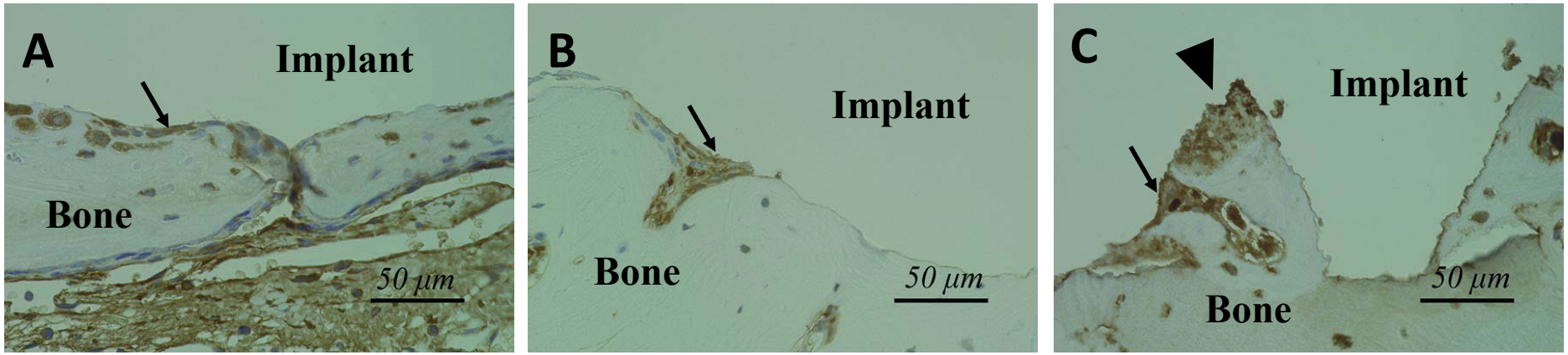

Figure 6. Immunohistochemical staining of osteoblast differentiation markers osteopontin (the upper part) and osteocalcin (the lower part)
Type A: no thread, Type B: macro-thread, and Type C: micro-thread
Positive proliferating cells are stained brown/black within the healing tissues near the implant-bone interface (arrow) especially in the valley of the micro-thread (arrow head). 40×

	3 weeks after implantation			8 weeks after implantation		
	Type A (n=2)	**Type B**	**Type C**	**Type A**	**Type B**	**Type C**
The number for osteopoetin (no./mm)	**20.17 ± 3.19**	**26.83 ± 2.64**	**28.50 ± 2.43**	**18.50 ± 1.64**	**16.00 ± 1.67**	**18.00 ± 2.53**
The numer for osteocalcin (no./mm)	**22.50 ± 6.29**	**18.00 ± 3.74**	**23.00 ± 5.83**	**15.67 ± 5.20**	**14.33 ± 4.50**	**17.00 ± 7.43**

Table 3 Number of osteoblasts at the interface of bone and implant stained by differentiation markers osteopontin and osteocalcin.

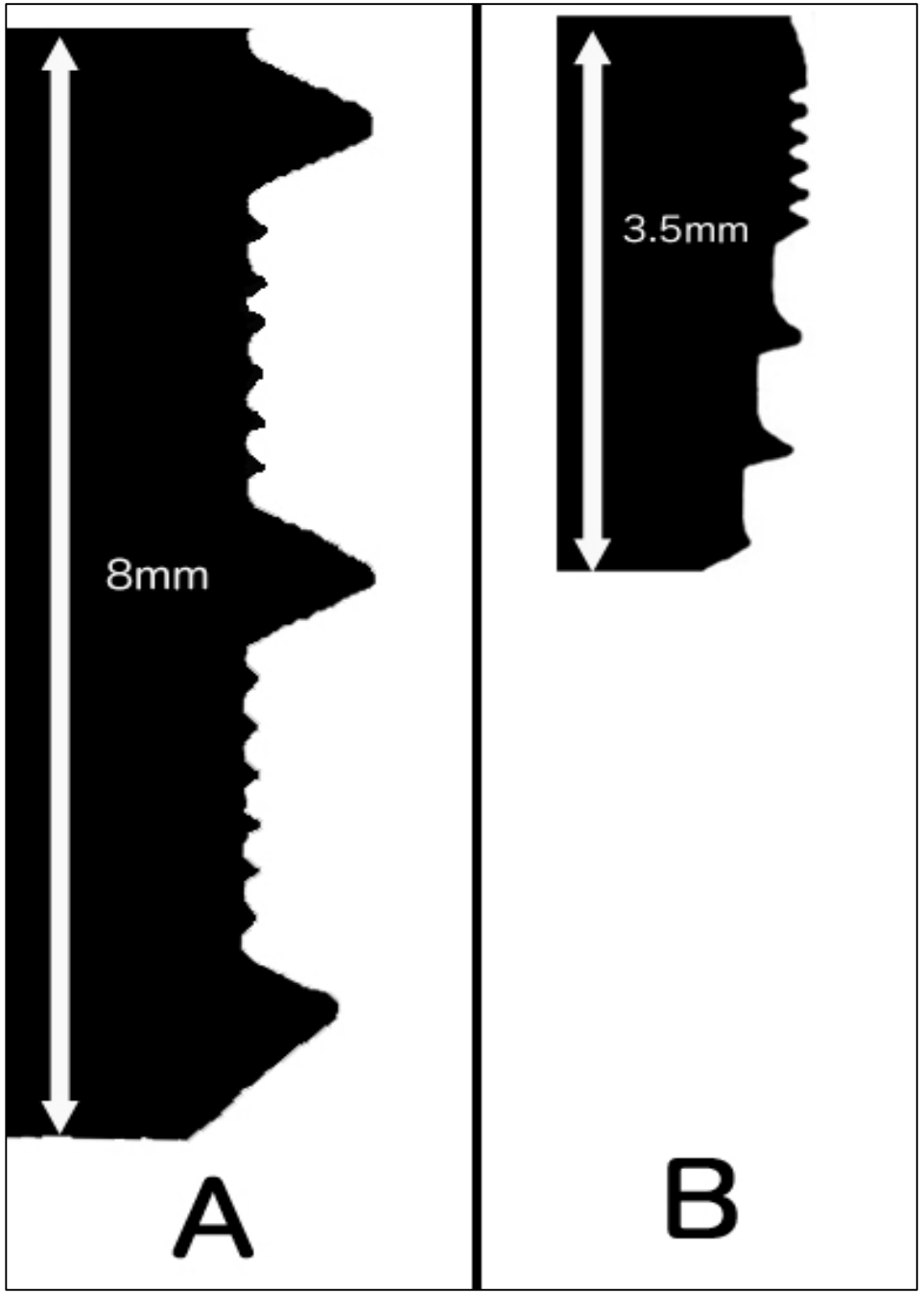

Fi**gure 7.** Macro- and micro-thread design employed in Chowdhary's study (A) and in this study (B)